

Preliminary Accuracy Evaluation of 3T MRI-guided Transperineal Prostate Biopsy with Grid Template

J. Tokuda¹, K. Tuncali¹, I. Iordachita², S-E. Song¹, A. Fedorov¹, S. Oguro¹, A. Lasso³, F. M. Fennessy¹, Y. Tang¹, C. M. Tempany¹, and N. Hata¹

¹Department of Radiology, Brigham and Women's Hospital, Boston, MA, United States, ²The Johns Hopkins University, Baltimore, MD, United States, ³School of Computing, Queen's University, Kingston, ON, Canada

Introduction MRI has been explored as an ideal tool to guide core needle biopsy of the prostate. The advantage of MRI over any other modality is its superior soft tissue delineation with various imaging techniques e.g. T1- and T2-weighted images, diffusion-weighted images and dynamic contrast-enhanced (DCE) images. Since early reports by D'Amico *et al.* demonstrated MRI-guided prostate transperineal biopsy using an open-configuration 0.5T MRI scanner [1], researchers' focus has been shifting from specially-designed scanners for better patient access to high-field closed-bore scanners for better image quality [2, 3]. Recent progress in magnet technologies allows the scanner vendors to design 3T closed-bore magnets with shorter and wider gantries that improve access to the patient without compromising image quality. This paper reports our preliminary accuracy evaluation of MRI-guided core needle biopsy of the prostate in a 70cm bore 3-Tesla MRI (Siemens Verio 3T, Siemens AG) using our specially-designed needle guidance template with a calibration frame and navigation software.

Materials and Methods Prostate Intervention Table: We designed and fabricated a prostate intervention table to support the patient in supine position in the MRI scanner. The prostate intervention table consists of 1) base board, 2) leg supports, 3) stationary frame and 4) grid template with a Z-shaped calibration frame (Z-frame) (Figure 1 a). The base board is a wooden plate placed on top of the patient table of the MRI scanner. The leg supports hold the patient's legs to secure the space between the thighs allowing the radiologist to access to the perineum from outside of the gantry (Figure 1 b). The grid template is an acrylic block (100×120×25 mm) with a grid of 1.3 mm holes spaced 5-mm apart, where the biopsy needles are inserted. The template is supported by a 2-degree-of-freedom adjustable holder, which allows shifting in the grid template in craniocaudal and anteroposterio direction. The Z-frame is attached to the template for registration of the grid template.

Registration of Grid Template by Z-frame: The grid template is registered to the image coordinate system by localizing the Z-frame in an MR image, after the grid template is fixed at the perineum of the patient. The Z-frame is made of 7 rigid tubes filled with MR-visible liquid and placed on three adjacent faces of a 60 mm cube. Those tubes are automatically detected in a cross sectional MRI image of the Z-frame providing the location and orientation of the Z-frame with respect to the image coordinate system. The MR imaging sequence we used was 3D FLASH (TR/TE: 12/1.97ms; matrix: 256×256×20; flip angle: 45°; pixel spacing: 0.63×0.63 mm; slice thickness: 2 mm; receiver bandwidth: 400 Hz/pixel; number of averages: 3). Once the grid template is registered, the Z-frame is detached from the grid template.

Navigation Software: We customized medical image processing and visualization software, 3D Slicer [4] to plan and guide the procedure. The customized software provides: (1) registration of pre- and intra-procedural images using B-spline non-rigid registration, (2) target planning based on the intra-procedural images and the registered pre-procedural images; (3) registration of the grid template by Z-frame; (4) selection of a hole on the grid template for the needle insertion based on the target location; (5) confirmation by MRI of the biopsy needle.

Clinical Study: We performed clinical prostate biopsies in the 3T MRI scanner. Five patients (age: 57-73) with suspected tumors in the prostate were enrolled. Once the patient was positioned at the isocenter, an image of the Z-frame was acquired with the abovementioned sequence for registering the grid template to the image coordinate system. While registering the grid template, a T2-weighted intra-procedural 2D multi-slice image of the prostate was acquired for planning using 2D TSE (TR/TE: 5250/100 ms; flip angle: 150°; matrix: 320×320; pixel spacing: 0.44×0.44 mm; slice thickness: 3 mm; receiver bandwidth: 205 Hz/pixel). We reviewed the intra-procedural T2w image to identify suspicious foci as biopsy targets on 3D Slicer. In addition, we register pre-procedural T2w image to the intra-procedural image using B-spline deformable image registration available in 3D Slicer to obtain the transformation between pre- and intra-procedural images. The transformation was then applied to pre-procedural images including DCE- and diffusion-weighted MRI acquired in the same imaging session as the pre-procedural T2w image, to define additional biopsy targets. The radiologist inserted a 18-gauge MRI-compatible core biopsy needle (E-Z-EM) through the hole selected by 3D Slicer with the calculated insertion depth. The position of the needle was then confirmed by axial images acquired at the planned target position with 2D FISP (TR/TE: 402/1.45 ms; flip angle: 48°; matrix: 128×128; pixel spacing: 1.56×1.56 mm; slice thickness: 6 mm; bandwidth: 1500 Hz/pixel). If the needle was found to be off the target, the needle was reinserted through a different hole. Upon satisfactory placement of the needle over the target, tissue was sampled and sent to a pathological examination. The accuracy of the needle placement was validated retrospectively by the distance between the center of the needle artifact in the 2D axial confirmation image and the planned target. Since the core biopsy needle cuts a core of tissue 20 mm long along the needle axis, we assumed that the error along the needle axis could be ignored.

Results The biopsy procedures were successfully performed in 5 cases. Table 1 summarizes the needle placement and its accuracy. Tissues were sampled from average 4 locations in 107 ± 15 minutes per case. Average number of cores was 7 per case and 26% of them were after reinsertions. The 2D root mean square errors (RMSE) between the needle and the planned targets before and after reinsertion were 4.9 mm and 4.6 mm respectively.

Discussion and Conclusion The targeting accuracy without reinsertion was less than the level of errors in an established MRI-guided clinical biopsy program using a grid template in a 0.5 T open-configuration MRI scanner, where the mean error in the targeted biopsy was 6.5 mm [5]. The comparison between the 2D RMSE of the needle placement before and after reinsertion indicates that reinsertion helped improving the accuracy. In conclusion, our preliminary accuracy evaluation demonstrated that it was feasible to perform prostate biopsy in the wide-bore 3T MRI scanner using the needle guidance template with the Z-frame and the navigation software.

Acknowledgements This work is supported by R01CA111288, P41RR019703, P01CA067165, U01CA151261, and U54EB005149 from NIH. Its contents are solely the responsibility of the authors and do not necessarily represent the official views of the NIH.

References [1] D'Amico AV *et al.*, J Urol, 2000; 164(2):385-387; [2] Susil RC *et al.*, Magn Reson Med 2004;52(3):683-687; [3] Hambrook T *et al.*, Invest Radiol 2008;43(10):686-694; [4] Gering DT *et al.*, J Magn Reson Imaging 2001; 13(6): 967-975; [5] Blumenfeld P *et al.*, J Magn Reson Imaging 2007;26(3):688-694.

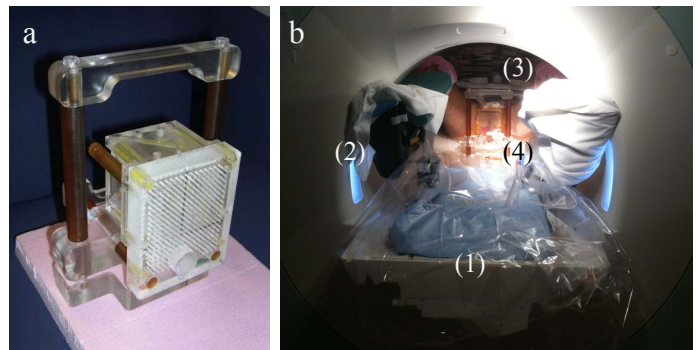


Figure 1. The photographs show the grid template with a Z-shaped calibration frame (Z-frame) (a) and the configuration of the prostate intervention table consisting of 1) base board, 2) leg support, 3) stationary frame and 4) grid template (b).

Table 1. Summary of needle placement in 5 clinical cases. The RMSE were obtained based on the distance between the center of the needle artifact and the expected needle position calculated from the holes on the template used for needle placement.

Case #	1	2	3	4	5
Number of target locations	2	3	5	4	6
Number of reinsertions	2	2	0	2	3
Total number of cores	4	6	8	6	11
RMSE before reinsertion (mm)	5.1	6.0	2.5	7.5	3.9
RMSE after reinsertion* (mm)	3.9	5.6	4.0	7.3	2.7
Duration of procedure (min)	105	100	110	90	130

* Including successful needle placement without reinsertion.